Vítor Monteiro, Andrés A. Nogueiras Meléndez, Carlos Couto, João L. Afonso

"Model Predictive Current Control of a Proposed Single-Switch Three-Level Active Rectifier Applied to EV Battery Chargers"

IEEE IECON Industrial Electronics Conference, Florence Italy, Oct. 2016.

http://ieeexplore.ieee.org/document/7793511/

ISBN: 978-1-5090-3474-1

DOI 10.1109/IECON.2016.7793511

Vítor Monteiro, Andrés A. Nogueiras Meléndez, Carlos Couto, João L. Afonso, "Model Predictive Current Control of a Proposed Single-Switch Three-Level Active Rectifier Applied to EV Battery Chargers", IEEE IECON Industrial Electronics Conference, Florence Italy, pp.1365-1370, Oct. 2016. DOI: 10.1109/IECON.2016.7793511 ISBN 978-1-5090-3474-1

Model Predictive Current Control of a Proposed Single-Switch Three-Level Active Rectifier Applied to EV Battery Chargers

Vítor Monteiro[1], Andrés A. Nogueiras Meléndez[2], Carlos Couto[1], João L. Afonso[1]
[1]ALGORITMI Research Centre – University of Minho, Guimarães – Portugal
[2]Departamento de Tecnología Electrónica – University of Vigo, Vigo – Spain
[1]{vitor.monteiro | carlos.couto | joao.l.afonso}@algoritmi.uminho.pt [2]aaugusto@uvigo.es

***Abstract*—This paper presents a model predictive current control applied to a proposed new topology of single-switch three-level (SSTL) active rectifier, which is exemplified in an application of single-phase battery charger for electric vehicles (EVs). During each sampling period, this current control scheme selects the state of the SSTL active rectifier that minimizes the error between the grid current and its reference. Using this strategy it is possible to obtain sinusoidal grid currents with low total harmonic distortion and unitary power factor, which is one of the main requirements for EVs chargers. The paper presents in detail the principle of operation of the SSTL active rectifier, the digital control algorithm and the EV battery charger (where is incorporated the SSTL active rectifier) that was used in the experimental verification. The obtained experimental results confirm the correct application of the model predictive current control applied to the proposed SSTL active rectifier.**

Keywords*—*Active Rectifier; Electric Vehicles; Model Predictive Current Control; Power Quality, Single-Switch.

I. INTRODUCTION

Nowadays, the electric vehicles (EVs) represent an important role in the transport sector and a real contribution to mitigate the greenhouse gases emissions [1]. In this context, with the spread of EVs, new challenges and opportunities are emerging. Some of them are related with the environmental and energy implications [2][3], new operation modes for the EVs integration in smart grids and smart homes [4][5], and the integration with renewables [6]. Besides, also the advances in terms of power electronics are relevant to strengthen the introduction of EVs [7][8].

The integration of EVs in the power grids should be performed considering power quality aspects, mainly, the reduced harmonic distortion of the grid current [9][10]. This issue is associated with the EV battery charging systems. Therefore, front-end active rectifiers has more notoriety when compared with the solutions based on diode rectifiers and multi-pulse rectifiers [11][12][13]. The main advantages of the active rectifiers is the possibility to control the grid current and the output voltage [11][14]. These rectifiers are identified in the literature as power-factor-correction (PFC) converters. Extensive revisions, respectively, about single-phase and three-phase active rectifiers are presented in [15] and [16]. The essence of three-phase active rectifiers is presented in [17] and [18]. Taking into account on-board EV battery charging systems, the main active rectifier is the well-known PFC converter that combines a diode-bridge rectifier with a dc-dc boost-type converter [19]. However, besides the boost converter can also be used other dc-dc converters, e.g., cuk, three-state switching cell, buck, buck-boost, and forward [20][21]. With the combining of two or more PFC converter it is possible to obtain interleaved PFC converters [22]. In this context, other important set of PFC converters are the multi-level [23][24] and the bridgeless [25], including the symmetrical and asymmetrical [26][27].

Fig. 1 shows the circuit topology of the proposed single-switch three-level (SSTL) active rectifier used in a single-phase battery charger for EV. Besides the inductive filter to couple the SSTL active rectifier to the power grid, it is also composed by a diode bridge rectifier (diodes D_1 to D_4) and by a bidirectional cell (IGBT S and diodes D_5 to D_8). A single-switch PFC active rectifier based in the Vienna converter is presented in [28], however, the dc-link is split and its nominal voltage should be, at least, the double of the maximum amplitude of the power grid voltage (the voltage in each capacitor is regulated in each half-cycle of the power grid voltage). This is the main drawback of this topology comparing with the SSTL active rectifier. In [29] and [30] are presented single-switch active rectifiers with high input power factor, however, without sinusoidal current consumption, i.e., with high current harmonic distortion, which represents the main disadvantage comparing with the SSTL active rectifier. New topologies of unidirectional three-level and five-level active rectifiers are presented, respectively, in [31] and [32]. However, they are more complex in terms of hardware and control than the SSTL. A comparative evaluation of PFC topologies for EV battery chargers based in the boost converter

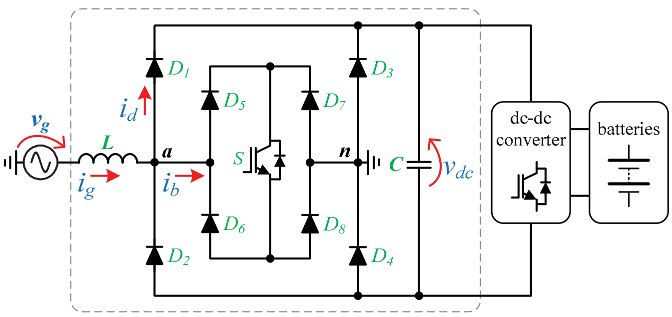

Fig. 1. Circuit topology of the single-switch three-level (SSTL) active rectifier for applications of battery chargers for electric vehicles (EVs).

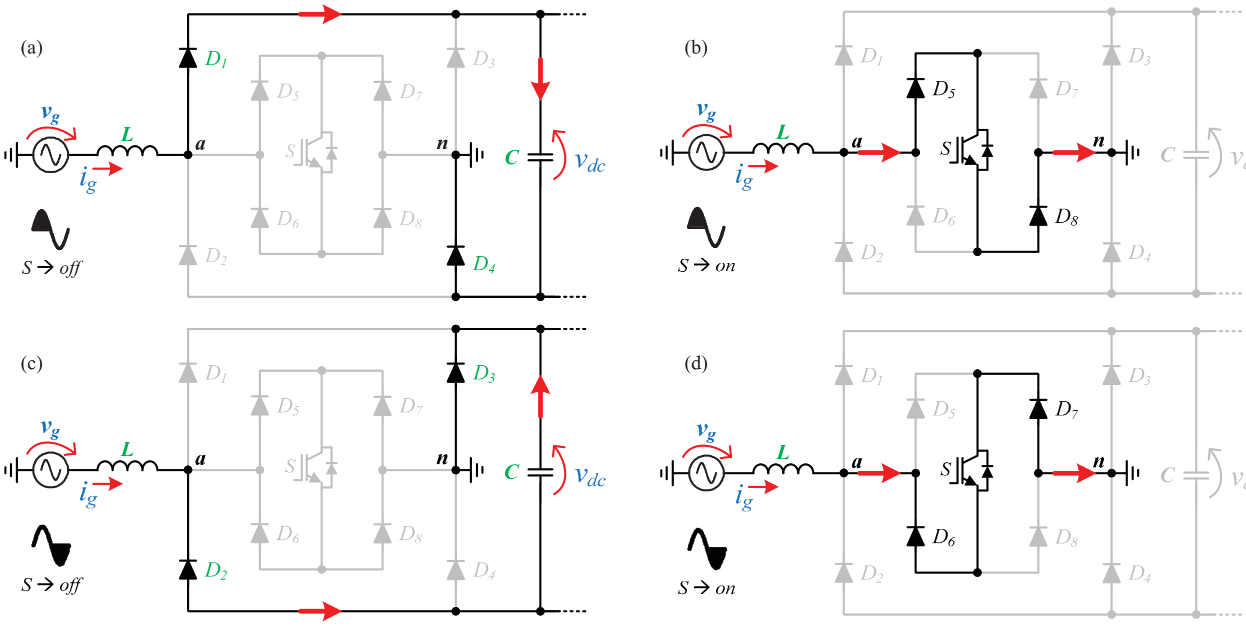

Fig. 2. Operation stages of the SSTL as active rectifier: (a)-(b) When $v_g > 0$; (c)-(d) When $v_g > 0$.

is presented in [33]. A detailed analysis of the SSTL active rectifier comparing with the traditional PFC (diode bridge rectifier with a dc-dc boost-type converter) is performed in section III.

The grid current control of the SSTL active rectifier is performed with the model predictive current control with finite control set [34]. This current control scheme uses the discrete-time model of the SSTL active rectifier and a cost function to minimize the error between the measured current and its reference, i.e., to define the state of the SSTL active rectifier during each sampling interval. The model predicitve current control scheme is presented in section II, while the analysis and the main simulation results are presented in section III. The experimental validation is presented in section IV and the main conclusions in section V.

II. Model Predictive Current Control Scheme

Fig. 2 shows the distinct stages used to define the state of the SSTL active rectifier during each sampling period. During the positive semicycle of the power grid voltage ($v_g > 0$), when the IGBT S is off the inductance provides energy and the voltage produced by the converter (v_{an}) is v_{dc}. When the IGBT S is on the inductance stores energy and the voltage produced by the converter (v_{an}) is 0. On the other hand, during the negative semicycle of the power grid voltage ($v_g < 0$), when the IGBT S is off the inductance provides energy and the voltage produced by the converter (v_{an}) is -v_{dc}. When the IGBT S is on the inductance stores energy and the voltage produced by the converter (v_{an}) is 0. Taking into account that the SSTL active rectifier should operate with a sinusoidal grid current, it can be seen as a linear load with unitary power factor. Therefore, the grid current is directly proportional to the power grid voltage according to:

$$i_g(t) = G_{EV}\, v_g(t)\,, \tag{1}$$

where, G_{EV} denotes a conductance that represents the SSTL active rectifier. This conductance is determined according to the mean value of the active power (P_{EV}) and the root mean square (rms) value of the power grid voltage (V_G) according to:

$$P_{EV} = G_{EV}\, V_G{}^2\,. \tag{2}$$

Substituting equation (1) into equation (2), the grid current reference for the SSTL active rectifier is obtained according to:

$$i_g{}^*(t) = \frac{P_{EV}}{V_G{}^2}\, v_g(t)\,, \tag{3}$$

where, the active power (P_{EV}) is established in function of the necessary power to charge the EV batteries through the dc-dc back-end converter. Taking into account that, typically, the batteries are charged with two distinct stages (constant current followed by constant voltage), the charging power is not constant. The maximum power occurs at the end of the first stage, where the batteries are charged with constant current and the battery voltage reaches the maximum value.

The model predictive current control scheme is based in the discrete-time nature of the SSTL active rectifier to define its state in each sampling interval. Analyzing the voltages and the current represented in Fig. 1 it can be established:

$$v_g(t) = L\frac{di_g(t)}{dt} + v_{an}(t)\,, \tag{4}$$

where, v_g denotes the instantaneous value of the power grid voltage, i_g the instantaneous value of the grid current, and v_{an} the voltage produced by the converter between the points a and n (cf. Fig. 1). Applying the forward Euler method to the derivative of the grid current, the discrete implementation of the equation (4) is obtained according to:

$$v_g[k] = \frac{L}{T_s}\big(i_g[k+1] - i_g[k]\big) + v_{an}[k]\,. \tag{5}$$

Rearranging equation (5) in order to the grid current, i.e., the variable that is controlled, is obtained:

$$i_g[k+1] = \frac{T_s}{L}\big(v_g[k] - v_{an}[k]\big) + i_g[k]\,. \tag{6}$$

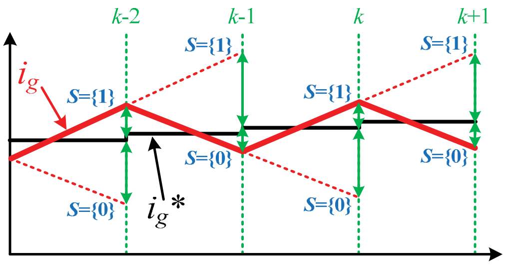

Fig. 5. Principle of operation of the SSTL active rectifier state selection.

TABLE I
SPECIFICATIONS OF THE EV BATTERY CHARGER

Parameters	Value	Unit
Nominal Grid Rms Voltage	230 ± 10%	V
Grid Frequency	50 ± 1%	Hz
Nominal Power	3.6	kW
Batteries Voltage	200 to 350	V
Nominal Batteries Current	10	A
Total Power Factor	0.99	-
Total Harmonic Distortion	<3%	-
Maximum Switching Frequency	20	kHz
Sampling Frequency	40	kHz

With the equation (6) the final stage of the model predictive current control is to minimize the error between the predicted current ($i_g[k+1]$) and its reference ($i_g*[k+1]$). According to [35], the reference of current in the instant $[k+1]$ can be extrapolated according by:

$$i_g{}^*[k+1] = 4i_g{}^*[k] - 6i_g{}^*[k-1] + \\ +4i_g{}^*[k-2] - i_g{}^*[k-3]\,. \tag{7}$$

The previous equations are calculated during each sampling interval and is used a cost function for minimizing the error defined by:

$$g[k+1] = \left\| i_g{}^*[k+1] - i_g[k+1] \right\|^2 . \tag{8}$$

According to equation (8), the error is zero when the cost function is zero. The principle of operation of the SSTL active rectifier state selection is shown in Fig. 5. As it can be seen, during each sampling interval (e.g., $[k, k+1]$) are two possibilities to define the SSTL active rectifier state (cf. Fig. 2), however is selected the state that minimizes the grid current error. It is important to note that during each sampling interval is selected only one of the possible states.

III. ANALYSIS AND SIMULATION RESULTS

In this section is presented an analysis of the SSTL active rectifier when compared with the traditional PFC active rectifier and are presented the main simulation results of the SSTL active rectifier. As aforementioned, the SSTL active rectifier is integrated with a dc-dc back-end converter in an EV battery charger. Table I shows the specifications of the EV battery charger. Fig. 3 shows the power grid voltage (v_g) and the grid current (i_g) compared with i_g* in a detail of 200 µs during the initial phase of the EV battery charging process. As shown, the grid current (i_g) increases slowly until the nominal value for the charging process without sudden variations contributing to preserve the power quality. This figure also shows in detail the grid current (i_g) and its reference (i_g*) aiming to verify that the grid current (i_g) tracks the reference (i_g*). Fig. 4 shows the power grid voltage (v_g) and the grid current (i_g) during a transient variation in the power, i.e., a

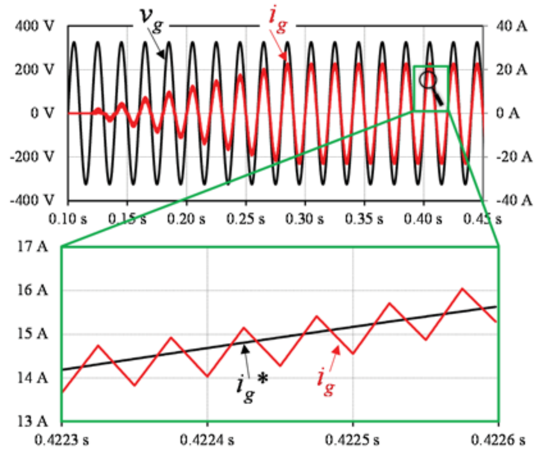

Fig. 3. Simulation results of the SSTL active rectifier during the initial phase of the EV battery charging process: Power grid voltage (v_g); Grid current (i_g); Grid current reference (i_g*).

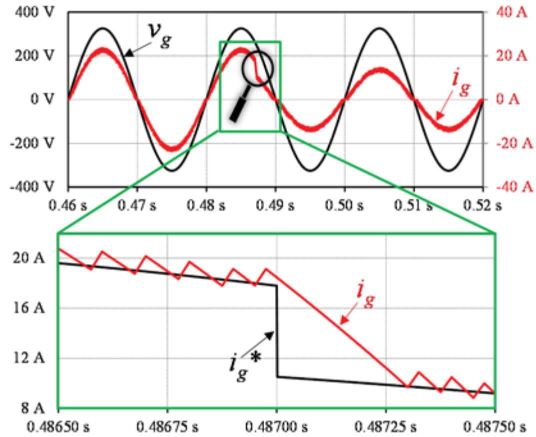

Fig. 4. Simulation results of the SSTL active rectifier during a transient variation in the power from 3.6 kW to 3 kW: Power grid voltage (v_g); Grid current (i_g); Grid current reference (i_g*).

reduction from 3.6 kW to 3 kW. This sudden variation corresponds to the transition from the first stage to the second stage of the EV battery charging process. This figure also shows in a detail of 100 µs the grid current (i_g) and its reference (i_g*) during the transient variation in the power. As it can be observed, the grid current (i_g) tracks the reference (i_g*) without sudden variations and with a delay of about 250 µs. Fig. 6 shows, in a detail of 600 µs, the grid current (i_g) the current in the diode bridge (i_d), the current in the bidirectional cell (i_b), and the control signal of the IGBT (v_S). Analyzing this figure, it is possible to observe that the grid current (i_g) is the sum of the current in the diode bridge (i_d) with the current in the bidirectional cell (i_b). During the positive semicycle of the power grid voltage ($v_g > 0$), the current in the diode bridge (i_d) corresponds to the stage when the IGBT S is off, the inductance provides energy, and the voltage produced by the converter is $+v_{dc}$. On the other hand, the current in the bidirectional cell (i_b) corresponds to the stage when the IGBT S is on, the inductance stores energy, and the voltage produced by the converter is 0. Using this strategy it is possible to reduce the rms value of the current in the diode bridge comparing to the traditional PFC active rectifier. Fig. 7 shows a comparison between the SSTL active rectifier and the traditional PFC active rectifier. The SSTL active rectifier uses more three diodes than the

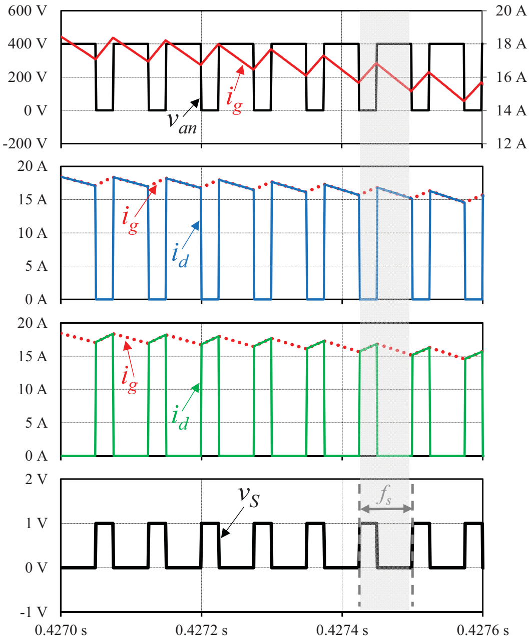

Fig. 6. Simulation results of the SSTL active rectifier in a detail of 600 µs: Grid current (i_g); Voltage produced by the SSTL active rectifier (v_{an}); Current in the diode bridge (i_d); Current in the bidirectional cell (i_b); Control signal of the IGBT (v_S).

traditional PFC, representing the main disadvantage, however, it has more advantages in terms of efficiency. In both active rectifiers, when the IGBT *S* is on, besides the IGBT are used two diodes, i.e., theoretically, the efficiency is equal. For the SSTL active rectifier, during the positive semicycle, are used the diodes D_5 and D_8, and during the negative semicycle are used the diodes D_6 and D_7. For the PFC, during the positive semicycle, are used the diodes D_1 and D_4, and during the negative semicycle are used the diodes D_2 and D_3. On the other hand, when the IGBT *S* is off, the SSTL active rectifier uses two diodes and the PFC uses three diodes, i.e., it is possible improve the efficiency of the SSTL active rectifier compared to the PFC. For the SSTL active rectifier, during the positive semicycle, are used the diodes D_1 and D_4, and during the negative semicycle are used the diodes D_2 and D_3. For the PFC, during the positive semicycle, are used the diodes D_1, D_4 and D_5, and during the negative semicycle are used the diodes D_2, D_3 and D_5. Table II presents a comparison between the traditional PFC and the SSTL active rectifier in terms of the rms current in the IGBT (I_S) and the rms current in the diode bridge (I_D). This comparison was established for a ranging power from 500 W to 3.5 kW. The value of the rms current in the IGBT *S* is the same for both cases, but the value of the rms current in the diode bridge is always lower with the SSTL active rectifier. From this analysis it can be concluded that the SSTL active rectifier uses more three diodes than the PFC (main disadvantage), but the nominal power of the diode bridge can be reduced once the rms current is always lower. These are the main reasons to adopt the SSTL active rectifier in detriment of the traditional PFC for the developed EV battery charger.

IV. Experimental Validation

This section presents the setup used to validate the SSTL active rectifier and the main experimental results obtained to confirm its operation. The experimental results were acquired

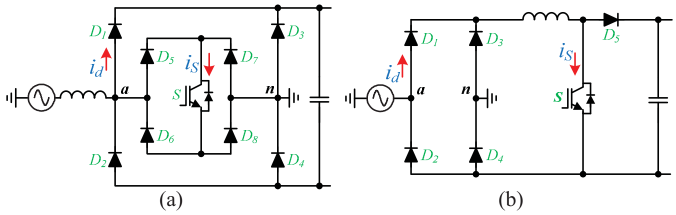

Fig. 7. Circuits of the active rectifiers compared in this paper: (a) SSTL active rectifier; (b) Traditional PFC.

TABLE II
RMS CURRENT COMPARISON BETWEEN THE TRADITIONAL PFC ACTIVE RECTIFIER AND THE SSTL ACTIVE RECTIFIER

Power	Rms I_S		Rms I_D	
	PFC	**SSTL**	**PFC**	**SSTL**
500 W	1.33	1.33	2.48	2.09
1000 W	2.53	2.53	4.64	3.89
1500 W	3.72	3.72	6.79	5.69
2000 W	4.93	4.93	8.97	7.49
2500 W	6.13	6.13	11.13	9.29
3000 W	7.36	7.36	13.33	11.11
3500 W	8.56	8.56	15.49	12.90

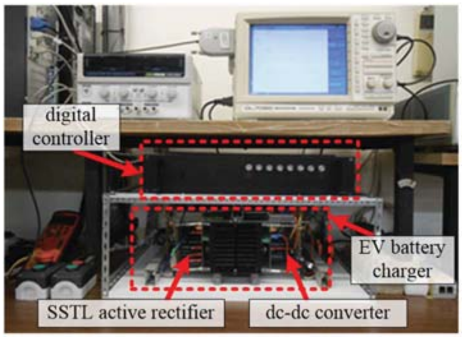

Fig. 8. Experimental setup of the EV battery charger where is incorporated the SSTL active rectifier combined with a dc-dc converter.

with a Yokogawa DL708E digital oscilloscope and with a Fluke 435 Power Quality Analyzer. Fig. 8 shows the experimental setup of the EV battery charger where is incorporated the SSTL active rectifier combined with the dc-dc converter. This figure also shows the digital control platform. Although the nominal grid voltage of the EV battery charger is 230 V, the experimental results were obtained with a voltage of 115 V. However, this operating voltage does not invalidate the experimental verification. It is important to note that the power grid voltage presents harmonic distortion (THD = 2.9%) due to the nonlinear electrical appliances and the line impedance. Taking into account that the SSTL is used in an EV battery charger, the experimental results were obtained only in steady state without sudden variations. Moreover, the beginning of the EV battery charging process is performed slowly, with the current increasing from zero to the nominal value. If occurs a voltage sag in the power grid, the control system will increase the current in order to maintain the dc-link voltage, however, this situation is not presented in the paper. The control algorithm is implemented in the fixed-point digital signal processor (DSP) TMS320F28335 from Texas Instruments. The power grid voltage is measured with the hall-effect LV-25 P sensor from LEM, and the EV current is measured using the hall-effect LA-55 P sensor also form LEM. Taking into account that these signals are bipolar (i.e., positive and negative), it is used a signal conditioning circuit to adapt these signals to the unipolar inputs of the analog-to-digital converters

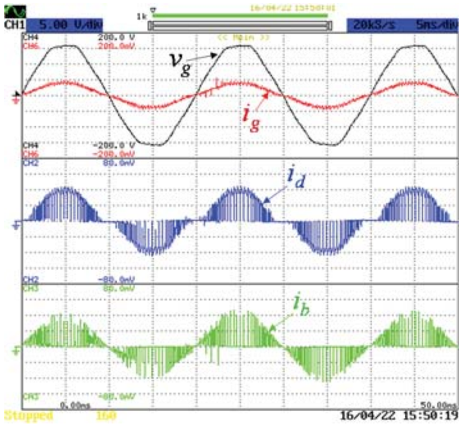

Fig. 9. Experimental results of the SSTL active rectifier: Power grid voltage (v_g: 50 V/div); grid current (i_g: 5 A/div); Current in the diode bridge (i_d: 2 A/div); Current in the bidirectional cell (i_b: 2 A/div).

(ADC) of the DSP. In order to connect the DSP and the IGBT driver is used a command circuit, i.e., a circuit used to adapt a signal of 3.3 V into a signal of 15 V. The IGBT driver is composed by the optocoupler HCPL3120 from Avago and by the isolated dc-dc source MEV1S1515SC from Murata. Besides the aforementioned circuits, is also used a protection circuit that disables the IGBT driver signal when the grid current reach the predefined threshold. This circuit deals with all the measured signal from the EV battery charger. The power converters of the EV battery charger are composed by the IGBTs FGA25N120ANTD from Fairchild. The dc-link is composed by a capacitor of 1000 µH (400 V) and the output LC filter of the dc-dc converter is composed by an inductor of 560 µH (10 A) and by a capacitor of 680 µF (400 V). The input filter of the SSTL active rectifier (5 mH) was designed with two cores T300-60D from Micrometals. Fig. 9 shows the power grid voltage (v_g), the grid current (i_g), the current in the diode bridge (i_d), and the current in the bidirectional cell (i_b). From this figure it is possible to observe that the grid current (i_g) is composed by the sum of the currents in the diode bridge (i_d) and in the bidirectional cell (i_b). During the positive semicycle of the power grid voltage ($v_g > 0$), Fig. 10 shows in detail the power grid voltage (v_g), the grid current (i_g), the current in the diode bridge (i_d), the current in the bidirectional cell (i_b), and the gate-emitter voltage of the IGBT (v_{ge}). Analyzing this figure, when the IGBT is on the current in the power grid (i_g) corresponds to the current in the bidirectional cell (i_b) and the current in the diode bridge (i_d) is zero, i.e., the inductance stores energy (cf. Fig. 2(a)). On the other hand, when the IGBT is off the current in the power grid (i_g) corresponds to the current in the diode bridge (i_d) and the current in the bidirectional cell (i_b) is zero, i.e., the inductance provides energy (cf. Fig. 2(b)). Fig. 11 shows the power grid voltage (v_g), the grid current (i_g), and the voltage produced by the SSTL active rectifier (v_{an}). As expected, the grid current (i_g) is sinusoidal and in phase with the power grid voltage (v_g), and the voltage produced by the converter (v_{an}) can assume three distinct values ($-v_{dc}$, 0, $+v_{dc}$). In this situation the measure total harmonic distortion (THD) of the power grid voltage was 2.9% and the THD of the EV current was 2.9%. Fig. 12 shows the spectral analysis and the THD of the EV current.

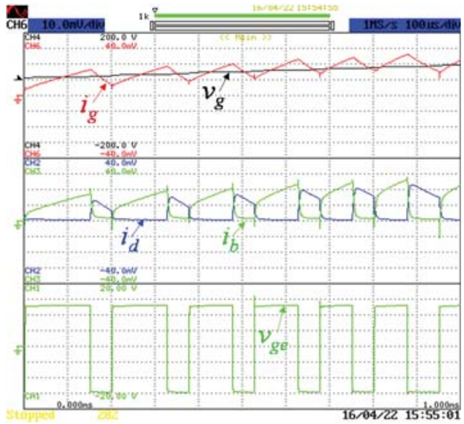

Fig. 10. Experimental results of the SSTL active rectifier: Power grid voltage (v_g: 50 V/div); grid current (i_g: 1 A/div); Current in the diode bridge (i_d: 1 A/div); Current in the bidirectional cell (i_b: 1 A/div); Gate-emitter voltage of the IGBT (v_{ge}: 15 V/div).

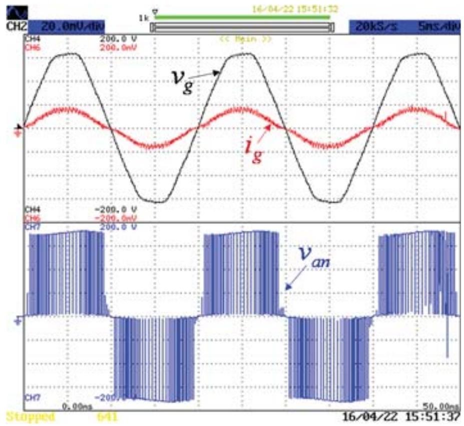

Fig. 11. Experimental results of the SSTL active rectifier: Power grid voltage (v_g: 50 V/div); Grid current (i_g: 5 A/div); Voltage produced by the SSTL active rectifier (v_{an}: 50 V/div).

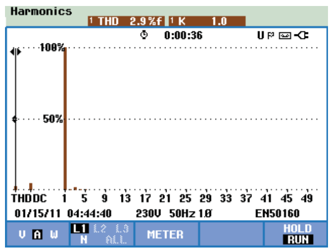

Fig. 12. Spectral analysis and THD of the grid current (i_g).

V. Conclusion

This paper proposes a new topology of single-switch three-level (SSTL) active rectifier for applications of battery chargers for electric vehicles (EVs), which is controlled by a model predictive current control. Along the paper is presented in detail the model predictive current control and the analysis of the principle of operation. The SSTL active rectifier was validated through simulations and experimental results, where the obtained results confirm the correct application of the model predictive current control to the SSTL active rectifier. The experimental results show that the control algorithm is suitable to obtain the three-level voltages and to track the reference of the grid current. The model predictive current control allows to follow the reference with low total harmonic distortion.

ACKNOWLEDGMENT

This work was supported in part by the FCT–Fundação para a Ciência e Tecnologia in the scope of the project: PEst-UID/CEC/00319/2013. Vítor Monteiro was supported by the scholarship SFRH/BD/80155/2011 granted by the FCT agency.

REFERENCES

[1] Ali Ipakchi, Farrokh Albuyeh, “Grid of the Future - Are we Ready to Transition to a Smart Grid?,” IEEE Power Energy Mag., vol.7, no.2, pp.52-62, Mar. 2009.

[2] Craig H. Stephan, John Sullivan, “Environmental and Energy Implications of Plug-In Hybrid-Electric Vehicles,” Environ. Sci. Technol. vol.42, no.4 pp.1185-1190, Jan. 2008.

[3] Álvaro Cunha, F. P. Brito, Jorge Martins, Nuno Rodrigues, Vitor Monteiro, João L. Afonso, “Assessment of the Use of Vanadium Redox Flow Batteries for Energy Storage and Fast Charging of Electric Vehicles in Gas Stations,” ELSEVIER Energy, 2016.

[4] Vítor Monteiro, J. G. Pinto, João L. Afonso, “Operation Modes for the Electric Vehicle in Smart Grids and Smart Homes: Present and Proposed Modes,” IEEE Trans. Veh. Tech., vol.65, no.3, pp.1007-1020, Mar. 2016.

[5] Vítor Monteiro, Bruno Exposto, João C. Ferreira, João Luiz Afonso, “Improved Vehicle-to-Home (iV2H) Operation Mode: Experimental Analysis of the Electric Vehicle as Off-Line UPS,” IEEE Trans. Smart Grid, 2016.

[6] Shuang Gao, K. T. Chau, Chunhua Liu, Diyun Wu, C. C. Chan, “Integrated Energy Management of Plug-in Electric Vehicles in Power Grid With Renewables,” IEEE Trans. Veh. Technol., vol.63, no.7, pp.3019-3027, Sept. 2014.

[7] Kaushik Rajashekara, “Present Status and Future Trends in Electric Vehicle Propulsion Technologies,” IEEE J. Emerg. Sel. Topics Power Electron., vol.1, no.1, pp.3-10, Mar. 2013.

[8] Murat Yilmaz, Philip T. Krein, “Review of Battery Charger Topologies, Charging Power Levels, and Infrastructure for Plug-In Electric and Hybrid Vehicles,” IEEE Trans. Power Electron., vol.28, no.5, pp.2151-2169, May 2013.

[9] Vítor Monteiro, João Paulo Carmo, J. G. Pinto, João L. Afonso, “A Flexible Infrastructure for Dynamic Power Control of Electric Vehicle Battery Chargers,” IEEE Trans. Veh. Technol., 2015 (accepted for publication).

[10] Vítor Monteiro, Henrique Gonçalves, João L. Afonso, “Impact of Electric Vehicles on Power Quality in a Smart Grid Context,” IEEE EPQU International Conference on Electrical Power Quality and Utilisation, pp.1-6, Oct. 2011.

[11] Bhim Singh, Brij N. Singh, Ambrish Chandra, Kamal Al-Haddad, Ashish Pandey, Dwarka P. Kothari, “A Review of Single-Phase Improved Power Quality AC-DC Converters,” IEEE Trans. Ind. Electron., vol.50, no.5, pp.962-981, Oct. 2003.

[12] Vítor Monteiro, Bruno Exposto, J. G. Pinto, M. J. Sepúlveda, Andrés A. Nogueiras Meléndez, João L. Afonso, “Three-Phase Three-Level Current-Source Converter for EVs Fast Battery Charging Systems,” IEEE ICIT International Conference on Industrial Technology, Seville Spain, pp.1401-1406, March 2015.

[13] Vítor Monteiro, J. G. Pinto, Bruno Exposto, João L. Afonso, “Comprehensive Comparison of a Current-Source and a Voltage-Source Converter for Three-Phase EV Fast Battery Chargers,” CPE International Conference on Compatibility and Power Electronics, Lisboa Portugal, pp.173-178, June 2015.

[14] Oscar García, José A. Cobos, Roberto Prieto, Pedro Alou, Javier Uceda, “Single Phase Power Factor Correction: A Survey,” IEEE Trans. Power Electron., vol.18, no.3, pp.749-755, May 2003.

[15] Bhim Singh, Brij N. Singh, Ambrish Chandra, Kamal Al-Haddad, Ashish Pandey, Dwarka P. Kothari, “A Review of Single-Phase Improved Power Quality AC-DC Converters,” IEEE Trans. Ind. Electron., vol.50, no.5, pp.962-981, Oct. 2003.

[16] Bhim Singh, Brij N. Singh, Ambrish Chandra, Kamal Al-Haddad, Ashish Pandey, Dwarka P. Kothari, “A Review of Three-Phase Improved Power Quality AC-DC Converters,” IEEE Trans. Ind. Electron., vol.51, no.3, pp.641-660, June 2004.

[17] Johann W. Kolar, Thomas Friedli, “The Essence of Three-Phase PFC Rectifier Systems—Part I,” IEEE Trans. Power Electron., vol.28, no.1, pp.176-198, Jan. 2013.

[18] Thomas Friedli, Michael Hartmann, Johann W. Kolar, “The Essence of Three-Phase PFC Rectifier Systems—Part II,” IEEE Trans. Power Electron., vol.29, no.2, pp.543-560, Feb. 2014.

[19] João Paulo M. Figueiredo, Fernando L. Tofoli, Bruno Leonardo A. Silva, “A Review of Single-Phase PFC Topologies Based on The Boost Converter,” IEEE INDUSCON International Conference on Industry Applications, pp.1-6, Nov. 2010.

[20] Huai Wei, Issa Batarseh, “Comparison of Basic Converter Topologies for Power Factor Correction,” IEEE Proceedings of Southeastcon, pp.348-353, Apr. 1998.

[21] Grover Victor Torrico-Bascopé, Ivo Barbi, “A Single Phase PFC 3 kW Converter Using a Three-State Switching Cell,” IEEE Power Electronics Specialists Conference, vol.5, pp.4037–4042, June 2004.

[22] Fernando Beltrame, Leandro Roggia, Luciano Schuch, José Renes Pinheiro, “A Comparison of High Power Single-Phase Power Factor Correction Pre-Regulators,” IEEE ICIT Industrial Technology, pp.625-630, Mar. 2010.

[23] José Rodríguez, Jih-Sheng Lai, Fang Zheng Peng, “Multilevel Inverters: A Survey of Topologies, Controls, and Applications,” IEEE Trans. Ind. Electron., vol.49, no.4, pp.724-738, Aug. 2002.

[24] Jih-Sheng Lai, Fang Zheng Peng, “Multilevel Converters-A New Breed of Power Converters,” IEEE Trans. Ind. Appl., vol.32, no.3, pp.509-517, May 1996.

[25] Laszlo Huber, Yungtaek Jang, Milan Jovanovic, “Performance Evaluation of Bridgeless PFC Boost Rectifier,” IEEE Trans. Power Electron., vol.23, no.3, pp.1381-1390, May 2008.

[26] Roberto Martinez, Prasad N. Enjeti, “A High-Performance Single-phase Rectifier with Input Power Factor Correction,” IEEE Trans. Power Electron., vol.11, no.2, pp.311-317, Mar. 1996.

[27] Jee-Woo Lim, Bong-Hwan Kwon, “A Power-Factor Controller for Single-Phase PWM Rectifiers,” IEEE Trans. Ind. Electron., vol.46, no.5, pp.1035-1037, Oct. 1999.

[28] Hani Vahedi, Philippe-Alexandre Labbé, Kamal Al-Haddad, “Single-Phase Single-Switch Vienna Rectifier as Electric Vehicle PFC Battery Charger,” IEEE VPPC Vehicle Power and Propulsion Conference, pp.1-6, Oct. 2015.

[29] Chien-Ming Wang, “A Novel Single-Switch Single-Stage Electronic Ballast With High Input Power Factor,” IEEE Trans. Power Electron., vol.22, no.3, pp.797-803, May 2007.

[30] Jong-Jae Lee, Jung-Min Kwon, Eung-Ho Kim,Woo-Young Choi, Bong-Hwan Kwon, “Single-Stage Single-Switch PFC Flyback Converter Using a Synchronous Rectifier,” IEEE Trans. Ind. Electron., vol.55, no.3, pp.1352-1365, Mar. 2008.

[31] André De Bastiani Lange, Thiago Batista Soeiro, Márcio Silveira Ortmann, Marcelo Lobo Heldwein, “Three-Level Single-Phase Bridgeless PFC Rectifiers,” IEEE Trans. Power Electron., vol.30, no.6, pp.2935-2949, June 2015.

[32] Vítor Monteiro, Andrés A. Nogueiras Meléndez, João C. Ferreira, Carlos Couto, João L. Afonso, “Experimental Validation of a Proposed Single-Phase Five-Level Active Rectifier Operating with Model Predictive Current Control,” IEEE IECON Industrial Electronics Conference, pp.3939-3944, Nov. 2015.

[33] Fariborz Musavi, Murray Edington, Wilson Eberle, William G. Dunford, “Evaluation and Efficiency Comparison of Front End AC-DC Plug-in Hybrid Charger Topologies,” IEEE Trans. Smart Grid, vol.3, no.1, pp.413-421, Mar. 2012.

[34] Marco Rivera, Venkata Yaramasu, Jose Rodriguez, Bin Wu, “Model Predictive Current Control of Two-Level Four-Leg Inverters—Part II: Experimental Implementation and Validation,” IEEE Trans. Power Electron., vol.28, no.7, pp.3469-3478, July 2013.

[35] Venkata Yaramasu, Marco Rivera, Bin Wu, Jose Rodriguez, “Model Predictive Current Control of Two-Level Four-Leg Inverters—Part I: Concept, Algorithm, and Simulation Analysis,” IEEE Trans. Power Electron., vol.28, no.7, pp.3459-3468, July 2013.